

Origin of Different Coordination Polyhedra for $\text{Cu}[\text{CF}_3\text{C}(\text{O})\text{CHC}(\text{O})\text{CF}_3]_2\text{L}$ ($\text{L} = \text{H}_2\text{O}, \text{NH}_3$)

Jiří Pinkas, John C. Huffman, Malcolm H. Chisholm,* and Kenneth G. Caulton*

Department of Chemistry and Molecular Structure Center, Indiana University,
Bloomington, Indiana 47405-4001

Received February 15, 1995[®]

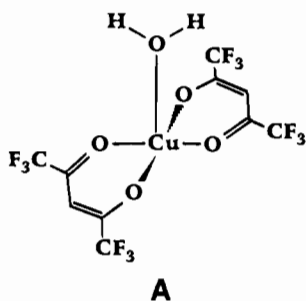
$\text{Cu}(\text{hfacac})_2(\text{NH}_3)$ ($\text{hfacac} = \text{CF}_3\text{C}(\text{O})\text{CHC}(\text{O})\text{CF}_3^-$) is shown to have a trigonal–bipyramidal structure with Cu–O (axial) = 1.945(3) Å, Cu–O (equatorial) = 2.075(3) Å and Cu–N = 1.933(6) Å. This contrasts with the square-pyramidal structure of $\text{Cu}(\text{hfacac})_2(\text{H}_2\text{O})$, which has a long (2.204(3) Å) Cu–OH_2 bond. The ammine complex retains its NH_3 ligand upon vacuum sublimation, while the H_2O complex loses water. The difference in coordination geometry and Cu–L distance ($\text{L} = \text{H}_2\text{O}, \text{NH}_3$) is traced to minimizing σ antibonding interactions with the stronger ligand L , which, by the criterion of $10Dq$, is NH_3 . Crystal data (-67°C): $a = 20.594(6)$ Å, $b = 8.881(2)$ Å, $c = 8.619(2)$ Å, $\beta = 104.49(1)^\circ$ with $Z = 4$ in space group $C2/c$.

Introduction

There is a general awareness of the easy interconversion between trigonal-bipyramidal and square-pyramidal structures, both leading to fluxionality and also to these two alternative structures being detectable as the ground state in slightly different environments. A classic example is the simultaneous occurrence of square-pyramidal and trigonal-bipyramidal forms of $\text{Ni}(\text{CN})_5^{3-}$ in the same unit cell.¹ A second example is the observation of the two forms in different polymorphs of the $\text{Co}(\text{dppe})_2\text{Cl}^+$ cation.²

The case of $\text{Cu}(\text{II})$, as the hfacac complex ($\text{hfacac} = \text{CF}_3\text{C}(\text{O})\text{CHC}(\text{O})\text{CF}_3^-$), is equally interesting. There is a large number of $\text{Cu}(\text{hfacac})_2\text{L}$ complexes with L a nitrogen or oxygen base. Even with two ligands L of apparently similar structures, there are cases where one structure is square-pyramidal and the other trigonal–bipyramidal.

We have reported earlier the structure³ of $\text{Cu}(\text{hfacac})_2(\text{H}_2\text{O})$, which is square-pyramidal (**A**) with an apical water ligand



attached at a rather long distance ($\text{Cu–O} = 2.204(3)$ Å). Consistent with this, this molecule melts around 135°C ⁴ and sublimates at $60\text{--}80^\circ\text{C}$ at 1×10^{-2} Torr with partial loss of water, to leave ultimately anhydrous $\text{Cu}(\text{hfacac})_2$.

[®] Abstract published in *Advance ACS Abstracts*, September 15, 1995.

- (1) Raymond, K. N.; Corfield, P. W. R.; Ibers, J. A. *Inorg. Chem.* **1968**, *7*, 1362.
- (2) Stalik, J. K.; Corfield, P. W. R.; Meek, D. W. *Inorg. Chem.* **1973**, *12*, 1668.
- (3) Pinkas, J.; Huffman, J. C.; Baxter, D. V.; Chisholm, M. H. *Chem. Mater.* **1995**, *7*, 1589.
- (4) (a) Belford, R. L.; Martell, A. E.; Calvin, M. J. *Inorg. Nucl. Chem.* **1956**, *2*, 11. (b) Bertrand, J. A.; Kaplan, R. I. *Inorg. Chem.* **1966**, *5*, 489.

We have reported earlier how the water protons can be an important participant in the chemical vapor deposition (CVD) chemistry which proceeds from $\text{Cu}(\text{hfacac})_2(\text{H}_2\text{O})$. We were interested in whether this neutral ligand influence carried over to the ammonia adduct $\text{Cu}(\text{hfacac})_2(\text{NH}_3)$. We report here the surprising result that this ammonia complex has a very different structure from that of the aquo adduct and that this difference has consequences for both the strength and lability of the Cu–L bond.

Experimental Section

$\text{Cu}(\text{hfacac})_2(\text{H}_2\text{O})$ was purchased from Aldrich and recrystallized from toluene to remove traces of $\text{Cu}_2(\text{OAc})_4 \cdot 2\text{H}_2\text{O}$. Methanol and acetonitrile for spectrophotometry were purchased from Fisher and Baxter, respectively. IR spectra were acquired on a Nicolet 510P FTIR spectrometer ($4000\text{--}400\text{ cm}^{-1}$) in KBr pellets. Mass spectra were run on a Kratos MS-80RFA high resolution instrument using EI mode at 30 eV and CI mode with methane ionizing gas. The masses are reported for the most abundant isotope present. UV–vis spectra were measured in the range 190–820 nm on a Hewlett-Packard 8452A diode array spectrophotometer in 1 cm quartz cells with a wavelength resolution of 2 nm. Elemental analyses were done by Atlantic Microlab. DSC measurements were done on a DuPont Model 2100 thermal analyzer under a flowing helium atmosphere (30 mL/min).

Synthesis of $\text{Cu}(\text{hfacac})_2(\text{NH}_3)$. $\text{Cu}(\text{hfacac})_2(\text{H}_2\text{O})$ (2.00 g, 4.04 mmol) was dissolved in 100 mL of dry toluene giving a blue-green solution. As gaseous NH_3 was bubbled through the solution for 3 min, a slightly exothermic reaction occurred and a bright blue precipitate was formed. The solid was filtered off, washed with 2×10 mL portions of toluene. Upon drying of the sample on a frit by a stream of air, the color gradually changed from blue to green. Additional drying for 24 h in vacuum afforded 1.78 g (89%) of $\text{Cu}(\text{hfacac})_2(\text{NH}_3)$. The product was sublimed at $55\text{--}70^\circ\text{C}$ at 1×10^{-2} Torr. Mp: $205.0\text{--}205.5^\circ\text{C}$. MS (EI, 30 eV), m/z (ion, relative intensity): 747 ($[\text{Cu}_2(\text{hfacac})_3]^+$, 25), 540 ($[\text{Cu}_2(\text{hfacac})_2]^+$, 57), 477 ($[\text{M} - \text{NH}_3]^+$, 53), 408 ($[\text{M} - \text{NH}_3 - \text{CF}_3]^+$, 100), 339 ($[\text{M} - \text{NH}_3 - 2\text{CF}_3]^+$, 68), 287 ($[\text{Cu}(\text{hfacac})\text{NH}_3]^+$, 28), 218 ($[\text{Cu}(\text{hfacac})\text{NH}_3 - \text{CF}_3]^+$, 17), 201 ($[\text{Cu}(\text{hfacac}) - \text{CF}_3]^+$, 65), 97 ($[\text{Cu}(\text{NH}_3)_2]^+$, 98), 80 ($[\text{Cu}(\text{NH}_3)]^+$, 59), 69 (CF_3^+ , 30). MS (CI, CH_4), m/z (ion, relative intensity): 557 ($[\text{Cu}_2(\text{hfacac})_2\text{NH}_3]^+$, 8), 540 ($[\text{Cu}_2(\text{hfacac})_2]^+$, 17), 495 ($[\text{M} + \text{H}]^+$, 3), 494 (M^+ , 2), 477 ($[\text{M} - \text{NH}_3]^+$, 46), 408 ($[\text{M} - \text{NH}_3 - \text{CF}_3]^+$, 58), 339 ($[\text{M} - \text{NH}_3 - 2\text{CF}_3]^+$, 47), 287 ($[\text{Cu}(\text{hfacac})\text{NH}_3]^+$, 20), 255 (12), 218 ($[\text{Cu}(\text{hfacac})\text{NH}_3 - \text{CF}_3]^+$, 8), 201 ($[\text{Cu}(\text{hfacac}) - \text{CF}_3]^+$, 97), 139 ($[\text{Hhfacac} - \text{CF}_3]^+$, 29), 82 (CuF^+ , 43), 69 (CF_3^+ , 100). UV–vis (CH_3CN) λ_{max} (log ϵ): 225 (3.88), 235 (sh), 286 (sh), 298 (sh), 308 (431), 328 nm (sh). IR (KBr pellet, $4000\text{--}400\text{ cm}^{-1}$): ν 3368 w ($\nu_{\text{as}} \text{NH}_3$),

Table 1. Crystallographic Data for Cu(hfacac)₂(NH₃)

chem formula	C ₁₀ H ₅ O ₄ NF ₁₂ Cu	space group	C2/c
a, Å	20.594(6)	T, °C	-67
b, Å	8.881(2)	λ, Å	0.710 69
c, Å	8.619(2)	ρ _{calc} , g cm ⁻³	2.153
β, deg	104.49(1)	μ(Mo Kα), cm ⁻¹	15.87
V, Å ³	1526.37	R ^a	0.0404
Z	4	R _w ^b	0.0412
fw	494.68		

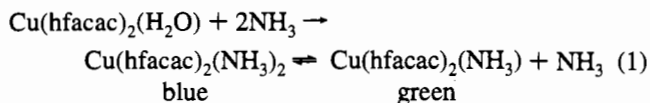
^a $R = \sum ||F_o| - |F_c|| / \sum |F_o|$. ^b $R_w = [\sum w(|F_o| - |F_c|)^2 / \sum w|F_o|^2]^{1/2}$ where $w = 1/\sigma^2(|F_o|)$.

3293 w (ν NH₃), 3226 vw, 3196 vw, 3148 w (ν CH), 1652 s (ν C=C), 1615 m (ν C=O), 1563 m, 1537 m, 1461 vs, 1350 vw, 1261 vs (ν_{as} CF₃), 1237 s (ν_s CF₃), 1212 vs, 1202 vs, 1144 vs (δ CH), 1112 w, 1087 w, 806 m (ν CCF₃), 769 w, 745 w, 675 m, 594 w, 586 w, 528 vw (ν Cu-O). Anal. Calcd for C₁₀H₅O₄NF₁₂Cu: C, 24.28; H, 1.02; N, 2.83. Found: C, 24.24; H, 1.16; N, 2.83. Single crystals suitable for X-ray experiments were grown from a saturated solution of Cu(hfacac)₂(NH₃) in ethanol/acetonitrile (20:1) at -20 °C.

X-ray Diffraction Structure Determination. A small, well-formed crystal was cleaved from a larger sample and affixed to the end of a glass fiber using silicone grease. The mounted sample was then transferred to the goniostat where it was cooled to -67 °C for characterization and data collection.⁵ Although the compound crystallizes as beautifully formed green crystals, initial attempts to mount a crystal were frustrating. The material is highly plastic and readily deforms when any force is applied. Since the crystals adhered to the glass container, it was difficult to obtain a suitable sample. When suitable crystals were finally obtained, it was discovered that the material also underwent a reversible phase transition. Although the exact temperature could not be ascertained, it is somewhere between -67 and -110 °C. A systematic search of a limited hemisphere of reciprocal space located a set of reflections with symmetry and systematic absences corresponding to one of two the monoclinic space groups *Cc* and *C2/c* (Table 1). Subsequent solution and refinement of the structure confirmed the centrosymmetric choice *C2/c*. Data were collected ($6^\circ < 2\theta < 45^\circ$) by using a standard moving-crystal, moving-detector technique with fixed background counts at each extreme of the scan. Data were corrected for Lorentz and polarization terms and equivalent data averaged. The structure was solved by direct methods (MULTAN78) and Fourier techniques. A difference Fourier map phased on the non-hydrogen atoms located all hydrogen atoms, although the three associated with the nitrogen are disordered. Attempts to refine the hydrogen atoms were unsuccessful, so they were placed in idealized positions for the final cycles of refinement. The molecule has crystallographic 2-fold symmetry. Attempts to refine the structure in *Cc* were unsuccessful. A final difference Fourier map was essentially featureless, the largest peak being 0.40 e/Å³. The results are shown in Tables 2 and 3 and Figures 1 and 2.

Results

Synthesis and Characterization. Cu(hfacac)₂(NH₃) was prepared by displacement of weakly-bonded water in Cu(hfacac)₂(H₂O) by ammonia according to eq 1. The blue color



of the product changed to green upon drying, thus attesting to an easy decomposition of presumably a diammine complex by a loss of one ammonia ligand. This behavior is reminiscent of aqua and pyridino systems Cu(hfacac)₂(L)_{*n*} (L = H₂O, py; *n* = 0, 1, 2).⁶ The color change was found to be reversible in ethanol solution. Electronic spectra of Cu(hfacac)₂(H₂O) (Table 4) show

Table 2. Fractional Coordinates^a and Isotropic Thermal Parameters^b for Cu(hfacac)₂(NH₃)

atom	10 ⁴ x	10 ⁴ y	10 ⁴ z	10B _{iso} , Å ²
Cu(1)	10000*	4346(1)	7500*	39
N(2)	10000*	6523(6)	7500*	38
O(3)	9223(1)	4349(4)	8399(4)	38
C(4)	8714(2)	3522(4)	7944(5)	24
C(5)	8580(2)	2413(5)	6803(5)	26
C(6)	9026(2)	2076(5)	5860(5)	26
O(7)	9563(1)	2707(3)	5854(3)	28
C(8)	8183(2)	3863(5)	8869(6)	31
F(9)	7643(1)	3009(3)	8437(3)	41
F(10)	8438(1)	3661(4)	10431(3)	48
F(11)	7987(1)	5291(3)	8665(4)	48
C(12)	8850(2)	752(6)	4700(5)	35
F(13)	9277(2)	-374(3)	5164(4)	54
F(14)	8891(2)	1160(4)	3246(3)	58
F(15)	8247(2)	198(4)	4552(3)	54

^a Parameters marked by an asterisk (*) are determined by symmetry. ^b Isotropic values for those atoms refined anisotropically are calculated using the formula given by: Hamilton, W. C. *Acta Crystallogr.* **1959**, *12*, 609.

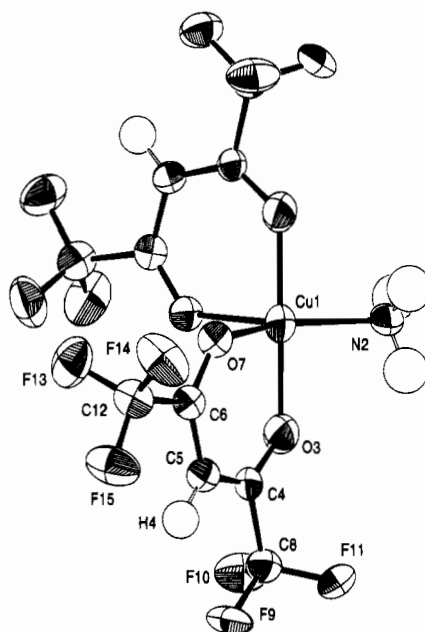

Figure 1. Molecular structure of Cu(hfacac)₂(NH₃). Unlabeled atoms are related to those labeled by a C₂ axis passing through Cu(1) and N(2).

Table 3. Selected Bond Distances (Å) and Angles (deg) for Cu(hfacac)₂(NH₃)

(a) Distances			
Cu(1)-O(3)	1.9447(25)	F(15)-C(12)	1.312(5)
Cu(1)-O(7)	2.075(3)	O(3)-C(4)	1.259(5)
Cu(1)-N(2)	1.933(6)	O(7)-C(6)	1.240(5)
F(9)-C(8)	1.320(5)	C(4)-C(5)	1.370(6)
F(10)-C(8)	1.330(5)	C(4)-C(8)	1.537(5)
F(11)-C(8)	1.329(5)	C(5)-C(6)	1.404(5)
F(13)-C(12)	1.326(6)	C(6)-C(12)	1.528(6)
F(14)-C(12)	1.328(5)		
(b) Angles			
O(3)-Cu(1)-O(3)'	179.88(20)	O(3)-Cu(1)-N(2)	89.94(10)
O(3)-Cu(1)-O(7)	90.79(12)	O(7)-Cu(1)-O(7)'	90.83(17)
O(3)-Cu(1)-O(7)'	89.30(13)	O(7)-Cu(1)-N(2)	134.58(9)

a band in the visible region which displays a blue shift upon saturation of the solution with ammonia. Similarly, the corresponding band in the spectrum of Cu(hfacac)₂(NH₃) shifts to the same λ_{max} after ammonia is bubbled through the solution. Evidently, the excess of ammonia drives the equilibrium in eq 1 to the side of the diammine adduct, and NH₃ is a stronger

(5) For a general description of diffractometer and crystallographic procedures, see: Huffman, J. C.; Lewis, L. N.; Caulton, K. G. *Inorg. Chem.* **1980**, *19*, 2755.

(6) Funk, L. L.; Ortolano, T. R. *Inorg. Chem.* **1968**, *7*, 567.

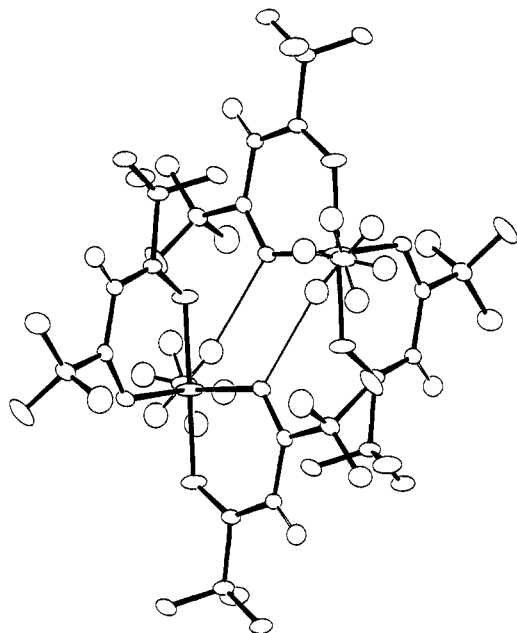


Figure 2. Diagram of $\text{Cu}(\text{hfacac})_2(\text{NH}_3)$ showing hydrogen-bonded dimeric units. This view is down the N–Cu bonds. Disorder is shown for the NH_3 hydrogens. The shortest intermolecular O/HN contacts are shown as open lines.

Table 4. Electronic Spectral Data for $\text{Cu}(\text{hfacac})_2(\text{L})_n$ in the Visible Region

$(\text{L})_n$	solvent	λ_{max} , nm	$\log \epsilon$
H_2O	MeOH	775	1.31
	CH_3CN	696	1.50
NH_3	MeOH	689	1.69
	CH_3CN	761	1.61
2NH_3	MeOH	642	1.87
	CH_3CN	649	1.92

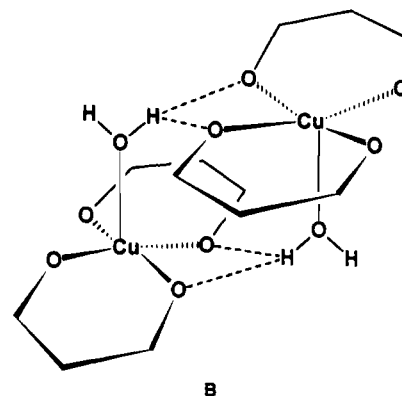
ligand than H_2O , methanol, or acetonitrile. $\text{Cu}(\text{hfacac})_2(\text{NH}_3)$ is very soluble in acetonitrile, acetone, and dimethylformamide, soluble in methanol and ethanol, and poorly soluble in aromatic and aliphatic hydrocarbons, Et_2O , chloroform, and CH_2Cl_2 . The monoammine complex sublimes intact at relatively mild conditions as was judged from constancy of its IR spectrum showing the NH stretches at 3368 and 3293 cm^{-1} . To compare the relative Cu–L (L = H_2O , NH_3) bond strengths in the two mono adducts in the gas phase, electron impact (30 eV) and chemical ionization (methane) mass spectra were measured. While EI ionization mode failed to reveal M^+ peaks for either of the two complexes, milder excitation by CH_5^+ provided weak M^+ and $[\text{M} + \text{H}]^+$ ions for the ammonia complex. The higher strength of the Cu–N bond corresponds well with the observed behavior under sublimation and also with the shorter Cu–N bond (see below) as opposed to the long Cu–O bond. In concert with our previous report, both complexes display, under either EI or CI conditions, the same higher mass fragments for dinuclear species such as $[\text{Cu}_2(\text{hfacac})_2]^+$.

We reported that $\text{Cu}(\text{hfacac})_2(\text{NH}_3)$ is also formed from anhydrous $\text{Cu}(\text{hfacac})_2$ and gaseous ammonia under CVD conditions used in preparation of Cu_3N .³ $\text{Cu}(\text{hfacac})_2(\text{NH}_3)$ has apparently been prepared by a reaction of Hhfacac in aqueous ammonia with CuCl_2 ;⁷ however, the authors incorrectly identified the product as $\text{Cu}(\text{hfacac})_2(\text{H}_2\text{O})_2$.

Structure of $\text{Cu}(\text{hfacac})_2(\text{NH}_3)$. The structure (Figure 1) reveals a monomer with rigorous C_2 symmetry; the C_2 axis passes through the Cu–N bond. All fluorines are ordered.

(7) Kidd, M. R.; Sager, R. S.; Watson, W. H. *Inorg. Chem.* **1967**, *6*, 946.

Consistent with the physical properties being different from those of the aquo adduct, the ammine and aquo adducts are *not* isomorphous. The X-ray study reveals molecules packed at essentially van der Waals contacts. The aquo adduct has hydrogen bonding as shown in B. Similarly, there is a weak

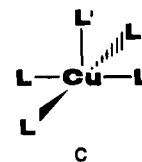


hydrogen bond ($\text{NH}\cdots\text{O} = 2.38 \text{ \AA}$, $\text{N-H}\cdots\text{O} = 166.1^\circ$) between N–H and one oxygen of a neighboring molecule, but the quantitative details of this interaction are obscured by the 2-fold disorder of the ammine hydrogens (Figure 2).

The surprising aspect of the molecular structure is that the molecule has a trigonal–bipyramidal form. Atoms O(3) and O(3)' comprise the axial direction and are within 1σ of being 180° apart. The three equatorial ligands and Cu are coplanar by symmetry, and the two independent equatorial angles are 134.6° (N–Cu–O) and 90.8° (O–Cu–O). The axial and equatorial Cu–O bond lengths are very different (0.130 \AA , or 26σ), and the Cu–N distance is short (e.g., as short as the shortest Cu–O distance).

Discussion

There is a huge body of structural data which reveals the tendency of Cu(II) to adopt varied coordination numbers, and even different geometries within coordination number 5.⁸ One description^{8c} of the data for five-coordinate species is in terms of the distance ρ (Å) from copper to the average plane of four ligands (C). As ρ goes from near zero to 0.5, the Cu–L' bond



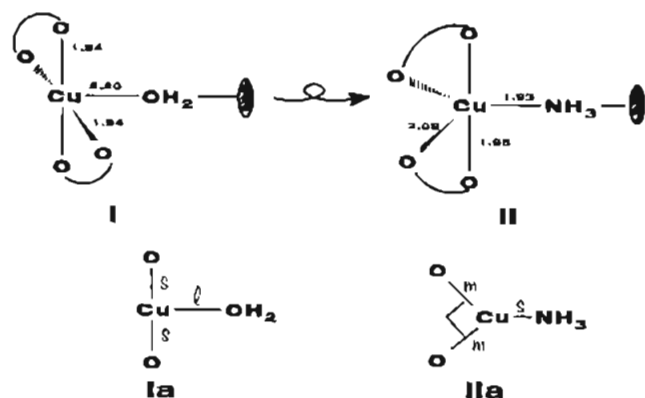
lengthens up to 0.4 \AA . Alternatively, for five *identical* ligands in $\text{Cu}^{\text{II}}\text{L}_5$ (L = NH_3 or Cl^-), (a) the axial Cu–L distances are 0.1 \AA shorter than the equatorial ones in a trigonal bipyramid (TBP) while (b) in a square pyramid (SP), the axial Cu–L distance is 0.15 \AA longer than the basal ones. Two other quantitative measures have been suggested for comparing real structural parameters to idealized limiting geometries on the Berry pathway, (i.e., a square pyramid and a trigonal bipyramid) and quantifying the degree of stereochemical distortion. The geometric parameter $\tau = 100(\beta - \alpha)/60$, where $\beta > \alpha$ are the trans angles not involving a unique ligand,⁹ adopts values from zero to 100% for perfectly tetragonal and trigonal-bipyramidal

(8) (a) Hathaway, B. J. *Struct. Bonding* **1984**, *57*, 55. (b) Sacconi, L. *Transition Met. Chem.* **1986**, *4*, 199. (c) Hathaway, B. J. *Coord. Chem. Rev.* **1987**, *5*, 594. (d) Hoskins, B. F.; Williams, F. D. *Coord. Chem. Rev.* **1972**, *9*, 365.

(9) Addison, A. W.; Rao, T. N.; Reedijk, J.; van Rijn, J.; Verschoor, G. *C. J. Chem. Soc., Dalton Trans.* **1984**, 1349.

geometries, respectively. Cu(hfacac)₂(H₂O) by this criterion ($\alpha = 167.0^\circ$, $\beta = 169.5^\circ$ ³) is only 4% distorted from the ideal square-pyramidal geometry. The value of $\tau = 149\%$ for Cu(hfacac)₂(NH₃) points to a "non-Berry" distortion of equatorial ligands which will be discussed below (i.e., two ligands have a mutual angle of less than 120°). For a comparison, the dihedral angle method^{10,11} was applied to our systems. The sum of differences of nine dihedral angles (formed by the normals to adjacent faces) of a real polyhedron and an ideal polyhedron was compared with the total change of these dihedral angles on going from the square pyramid to the trigonal bipyramid. In an agreement with the τ -index, Cu(hfacac)₂(H₂O) displays a 3% average distortion from the square-pyramidal stereochemistry while Cu(hfacac)₂(NH₃) again shows a "non-Berry" geometry with a distortion from the square pyramid of 146%. We present here some arguments which contribute an understanding of these observations. The orbital patterns for TBP and SP are clearly described,¹² but that paper does not focus on the d⁹ configuration and the existing data for Cu^{II}L₅ (particularly for the square pyramid) to the extent that we do here.

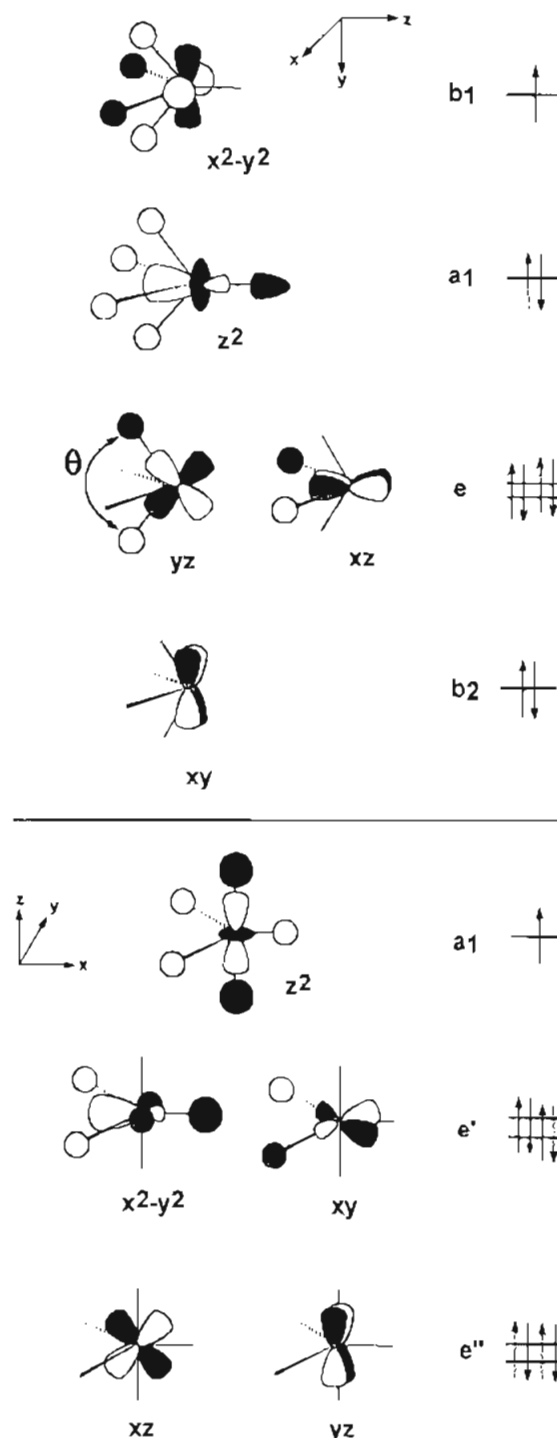
The fundamental differences between the structures of Cu(hfacac)₂L for L = H₂O and L = NH₃ can be summarized as follows: two Cu—O distances involving those oxygens which bend away from L lengthen markedly and the Cu—L distance¹³ shortens dramatically when H₂O is replaced by NH₃. This is nicely illustrated by drawings I¹⁴ and II.¹⁵ Note that there are



no other fundamentally important changes on replacement of water by ammonia: hydrogen bonding to hfacac oxygens is not altered. Since the changes are localized in one plane, the simplified drawings Ia and IIa are useful (s = short, m = medium, l = long).

One way to understand these differences is to recognize that both molecules are 19-electron complexes. Thus, antibonding metal-centered orbitals are occupied, and some bonds will therefore be long. The difference is then that this antibonding effect is concentrated on OH₂ in I, whereas it is apparently concentrated toward the (more distant) equatorial hfacac oxygens in II. Note that the axial hfacac oxygens in II undergo no significant change relative to the corresponding values in I. Note also that the Cu—O(hfacac) distances in II are not lengthened as much (they are thus "medium") as the Cu—OH₂ distance in

Chart 1



I, apparently since the antibonding influence of the one electron is diluted over two Cu—O bonds.

It is also possible to rationalize this effect more specifically by looking at the orbital occupancies of the frontier (metal-centered d) orbitals and considering effects of σ and, in the case of H₂O ligand, π repulsive interactions. The qualitative MO diagrams (Chart 1) were derived for idealized C_{4v} and D_{3h} symmetries of I and II, respectively.¹² First, we examine the σ -bonding framework in I and II. The orbital pattern for I has z² doubly occupied, so the full antibonding effect (i.e., z² is strongly σ^* (M—OH₂) in character) is felt by one ligand, and thus the axial ligand shows a long bond. On the other hand, the repulsive effect of five antibonding electrons in (primarily) x² - y² and (to a lesser extent) xz, yz is spread over four Cu—O

(10) Muetterties, E. L.; Guggenberger, L. J. *J. Am. Chem. Soc.* **1974**, *96*, 1748.

(11) Holmes, R. R.; Deiters, J. A. *J. Am. Chem. Soc.* **1977**, *99*, 3318.

(12) Rossi, A. R.; Hoffmann, R. *Inorg. Chem.* **1975**, *14*, 365.

(13) Orpen, A. G.; Brammer, L.; Allen, F. H.; Kennard, O.; Watson, D. G.; Taylor, R. *J. Chem. Soc., Dalton Trans.* **1989**, S1.

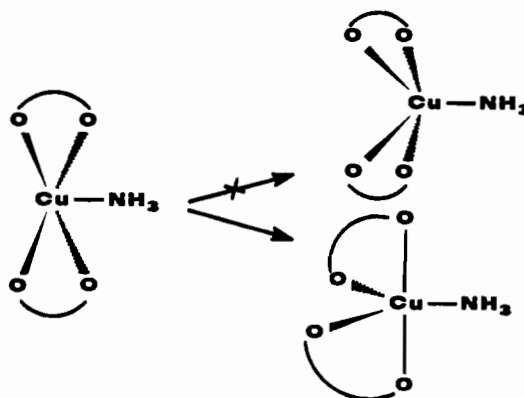
(14) For comparison, Cu(3-Meacac)₂ is planar with a 1.91 Å Cu—O distance: Robertson, J.; Truter, R. *J. Chem. Soc. A* **1967**, 309.

(15) For comparison, [Cu(hfacac)₂]₂(μ -pyrazine) is square-pyramidal with Cu—N = 2.248(6) Å and an average Cu—O = 1.951(6) Å: Romero, R. R.; Porter, L. C. *Acta Crystallogr.* **1993**, *C49*, 1487.

basal bonds, which is manifested in shorter basal bond lengths. Moreover, antibonding character of the xz , yz set is strongly dependent on the degree of pyramidity of the basal bonds (defined by angle θ). A flatter CuO_4 basal array diminishes the antibonding character of these orbitals (i.e., they are only of π -symmetry to O), which in turn strengthens the basal bonds. The values of θ for **I** ($169.5(1)$ and $167.0(1)^\circ$ ³) agree with the predicted angle range 165 – 180° for stronger basal bonds.¹² The two d electrons in xy have no effect of geometry as they reside in a strictly nonbonding metal-based orbital.

In **II**, there is a crucial change in that $x^2 - y^2$ and z^2 have occupancies opposite from those in **I**. In **II**, only approximately half of the amplitude of the (now doubly-occupied) $x^2 - y^2$ orbital (i.e., the x^2 part) operates on the NH_3 ligand compared to what operated on the aquo ligand in **I**. Moreover, the two axial oxygen ligands in **II** suffer only a singly-occupied σ^* orbital (the z^2), while the equatorial ligands feel primarily the doubly-occupied strongly antibonding σ^* (Cu-O equatorial) orbital xy . It is therefore clear that the equatorial Cu-O distances in **II** should be longer than the axial ones and that the neutral ligand in **II** should have a shorter Cu-L bond than the neutral ligand in **I**. This conclusion follows for any primarily σ donor ligand L in a square pyramid *vs* a trigonal bipyramid. An examination of available structural data supports this conclusion.⁸

The second important factor governing the bond lengths is repulsive interactions of filled metal-based orbitals of π symmetry with π -type lone pairs on the ligands L. While ammonia is only a σ donor, water can act as both a σ and a single-faced π donor. In the apical site of a square-pyramidal complex, the water was found having a planar oxygen; thus the π lone pair faces a filled doubly degenerate (e) set of π -type orbitals xz and yz . This presumably also contributes to the elongation of the apical bond. In the event that the geometry of the aquo adduct were trigonal pyramidal, the lone pair would encounter a very strong repulsion from xy and xz filled orbitals. Of the four possible π -type repulsive interactions, with xz and yz in the square-pyramidal and xz and xy in the trigonal-bipyramidal complex, the xy of the latter geometry is the strongest. This partially explains the preference of H_2O for the tetragonal arrangement. One can also argue that ammonia disfavors the square-pyramidal complex for the following reason. As it was noted above, the filled z^2 orbital strongly repels an apical substituent by a σ^* interaction. The energy of this antibonding orbital is related to a pyramidity of the basal ligand array and decreases on going to a more pyramidal geometry. Thus, a way to relieve this unfavorable repulsion is to displace the copper atom from the oxygen square-planar array toward nitrogen and to close the O-Cu-O angles. However, rigidity of the hfaccac ligand probably hinders this process and resists closing of the ligand bite angle. This leads to a collapse of the tetragonal array into a trigonal-bipyramidal structure. Further decrease of the Cu-N antibonding σ repulsion can be accomplished by



closing the equatorial O-Cu-O angle from 120° which stabilizes the $x^2 - y^2$ orbital.¹⁶ This was observed in the molecular structure of **II** where the angle is 90.8° .

What really remains to explain then is *why* NH_3 and H_2O elicit different coordination geometries of Cu(II) in **I** and **II**. The parameter $10Dq$, which is a measure of σ -bonding effectiveness for the (nearly pure) σ ligands H_2O and NH_3 , is larger (by about 25%)¹⁷ for NH_3 than for water. This means that the σ^* influence weakening the Cu-axial ligand bond in structure **I** will be more acute for NH_3 than for H_2O . We suggest that this contributes significantly to the geometry change and that strong σ -donor ligands in general will avoid the square-pyramidal structure.

Impact of Structure on Adduct Stability. What is noteworthy is the fact that the observed structural change, and in particular the consequent short and strong bond to ammonia, correlates well with the fact that, while the water adduct dehydrates significantly during vacuum sublimation (primarily $\text{Cu}(\text{hfaccac})_2$ deposits on the cold finger), the ammonia adduct sublimes intact. It is remarkable that a structural change correlates so dramatically with distinct physical properties and specifically with the relative kinetic lability of the Cu-L bond. It is also true that the melting point of the ammonia adduct (melts reversibly at 205°C) is much higher (and better defined) than that of the water adduct, which melts at 135°C .¹⁸ Finally, the crystals of the ammonia adduct are quite easily deformed on handling (i.e., plastic), while crystals of the aquo adduct have apparently normal "hardness".

Acknowledgment. This work was supported by the Department of Energy (Grant DE-FG02-90ER45427) through the Midwest Superconductivity Consortium.

Supporting Information Available: Full tables of crystallographic details and anisotropic thermal parameters (2 pages). Ordering information is given on any current masthead page.

IC950176F

(16) Rachidi, I. E.; Eisenstein, O.; Jean, Y. *New J. Chem.* **1990**, *14*, 671.

(17) Figgis, B. N. *Introduction to Ligand Fields*; Wiley-Interscience: New York, 1966; p 242.

(18) This melting behavior was confirmed by DSC measurements.